Theoretical Determination of the Electronic Mechanisms of 1,3-Dipolar Cycloaddition Reactions of Fulminic Acid and Diazomethane

Shogo Sakai*,† and Minh Tho Nguyen*,‡

Department of Applied Chemistry, Faculty of Engineering, Gifu University, Yanagido, Gifu 501-1193, Japan, and Department of Chemistry, University of Leuven, Celestijinenlaan 200F, B-3001 Leuven, Belgium

Received: April 20, 2004; In Final Form: August 15, 2004

The electronic mechanisms of 1,3-dipolar cycloaddition reactions of fulminic acid (ONCH) and diazomethane ($NNCH_2$) with HC≡CH, N≡CH, and P≡CH are studied using ab initio molecular orbital methods. The reaction mechanisms can be classified into two classes: ionic electrocyclic and diradical coupling mechanisms. Ionic electrocyclic mechanism occurs in reaction systems with a large difference in electronegativities between the two atoms of the dipolarophile and their atoms react with the atoms with each opposite charge of a 1,3-dipole. Diradical coupling mechanism occurs through two processes: the first process is a one-electron movement from the edge atom to the center atom of a 1,3-dipole, which leads to a biradical state (for ONCH, the one-electron movement occurs from the oxygen to the nitrogen atom; for $NNCH_2$, the movement occurs from the carbon to the center nitrogen atom). The second process is the breaking of the π-bond of the dipolarophile, which is strongly associated with the activation energy, followed by the formation of the new σ-bond (cyclic reaction) through concerted or stepwise modes.

1. Introduction

1,3-Dipolar cycloaddition (1,3-DC) is a powerful approach for synthesizing five-membered heterocyclic compounds.[1,2] In general, the reaction is assumed to proceed through a concerted [$\pi_{4s} + \pi_{2s}$] pericyclic addition,[3−5] similar to that of a Diels−Alder reaction.[6−8] This reaction follows the usual spin-coupled pattern of a bond-breaking/bond-forming process, as described in Scheme 1. However, for the electronic mechanism of the concerted 1,3-DC of fulminic acid to acetylene, on the basis of valence bond and molecular orbital theories, three electronic mechanisms have been recently proposed by four groups.[9−13] Leroy and co-workers[14−16] proposed a mechanism based on the evolution of Boys localized orbitals (LMO) along the minimum energy path (Scheme 1, mechanism II). Accordingly, the oxygen and carbon atoms of fulminic acid were assigned as the new bond donor and acceptor, respectively. In 1998, Karadakov, Cooper, and Gerratt[13] reconsidered the mechanism of the HCNO + HCCH system using the valence bond approach in its modern spin-coupled form. In accordance with mechanism II, the orbital pairs that correspond to the three distinct bonds of the reactants (in-plane C−C, C−N, and N−O bonds) shift simultaneously to create the two new bonds (closing the ring) and a nitrogen lone pair. Subsequently, Nguyen, Chandra, Sakai, and Morokuma[12] analyzed the electron reorganization along the reaction path by the configuration interaction−localized molecular orbital−complete active space (CI/LMO/CAS; CiLC) analysis[17−21] and the density functional theory based reactivity descriptors such as the Fukui function and local softness.[22,23] Analysis using CiLC showed that the addition starts with an electron migration from the oxygen to the nitrogen atom within the HCNO moiety, and ends with the carbon and the oxygen as the new bond donor and acceptor centers, respectively. This electronic movement is also consistent with that derived from the reactivity descriptors

SCHEME 1

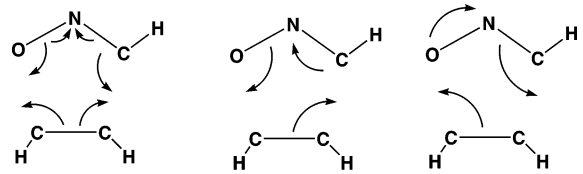

SCHEME 2

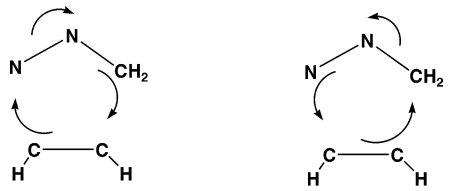

suggesting that, in the case of HCNO, the carbon atom bears a larger *f* value than the oxygen atom (Fukui function for electrophilic attack being an indicator for the electron donation ability). Thus, three distinct viewpoints on the electronic mechanism of the HCNO + HCCH reaction have been obtained, depicted as mechanisms I, II, and III in Scheme 1.

In the case of the 1,3-DC of diazomethane ($NNCH_2$) to ethylene, a 1975 LMO analysis by Leroy and Sana[24] has shown that the carbon and nitrogen ends of $NNCH_2$ play the roles of the σ-bond donor and acceptor, respectively (mechanism IV, Scheme 2) and that the lone pair of the central nitrogen results from the N≡N triple bond upon the bending of the CNN skeleton. In contrast, a study by Karadakov et al. in 2001,[25] as depicted in mechanism V of Scheme 2, suggested a completely opposite direction of the electron flow, in which the carbon and nitrogen atoms of the $NNCH_2$ molecule are the σ-bond acceptor

† Gifu University. E-mail: sakai@apchem.gifu-u.ac.jp.
‡ University of Leuven. E-mail: minh.nguyen@chem.kuleuven.ac.be.

10.1021/jp048275e CCC: $27.50
Published on Web 09/25/2004

and donor, respectively, and that the central nitrogen lone pair is formed from the C═N bond. In view of such a disagreement, we describe herein our attempt to clarify the electronic mechanism for these 1,3-DC's, in which the following 10 systems of 1,3-dipolar reactions were analyzed using the CiLC−IRC method.

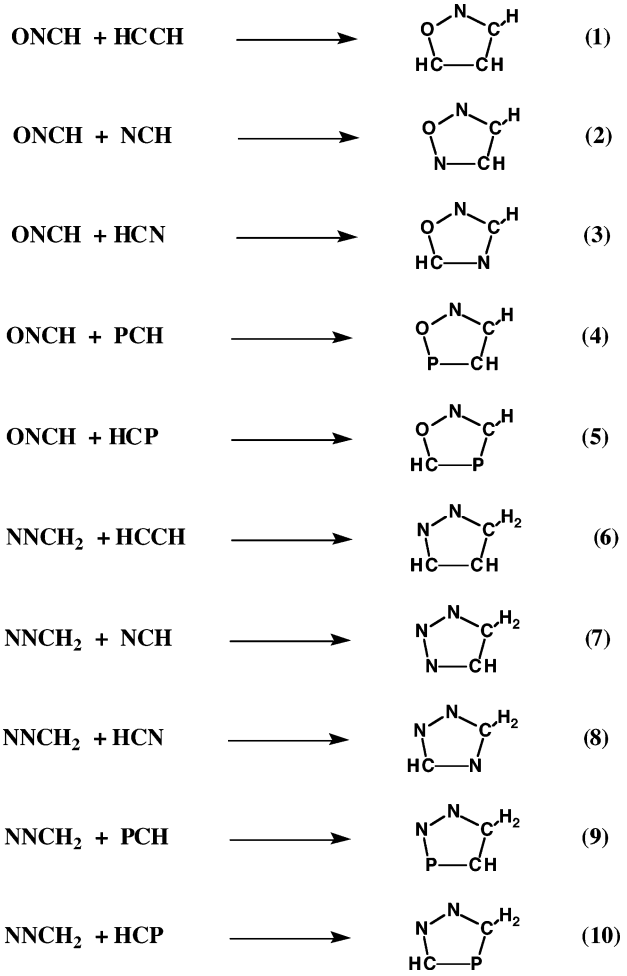

2. Methods

For all 10 reaction systems, the equilibrium geometries of the reactants, products, and transition structures were determined with analytically calculated energy gradients using the complete active space (CAS) self-consistent-field (SCF) method,[26] following initial calculations using density functional theory with the 6-31G(d) basis set.[27,28] For the CASSCF calculations, five active orbitals and six electrons were selected, and all configurations in the active spaces were generated. The five-orbitals active space corresponds to three p-orbitals on the molecular plane of 1,3-dipoles (HCNO and $NNCH_2$) moiety of the reaction system and two p-orbitals on the molecular plane of the dipolarophiles (HCCH, NCH, and PCH). These five orbitals relate to the bond forming and breaking process. Additional calculations were performed to obtain improved energy comparisons: the energy calculations at the CASSCF-optimized structures with electron correlation incorporated through the multiconfigurational second order Mϕller−Plesset perturbation theory (CAS-MP2).[29] Calculations using singles and doubles coupled-cluster theory with perturbative corrections for triples (CCSD(T))[30] were also performed using the CASSCF-optimized geometries in conjunction with the aug-cc-pVTZ basis set.[31−33] The density functional employed was the Becke's three parameter nonlocal exchange functional with the Lee, Yang, and Parr correlation function (B3LYP).[34,35] The intrinsic reaction coordinate (IRC)[36,37] was followed from the transition structure toward both the reactants and the products at the CASSCF level.

SCHEME 3

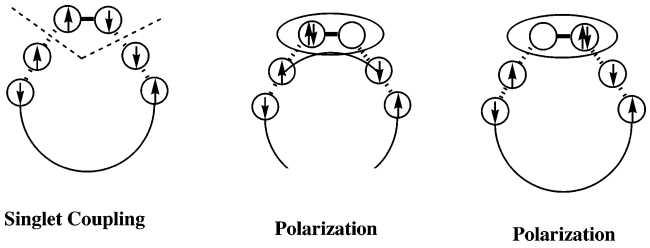

To interpret the electronic mechanisms of the reaction processes, configuration interaction (CI) localized molecular orbital (LMO)-CASSCF analyses were carried out according to a method described in detail elsewhere[17−21,38−43] using the 6-31G(d) basis set. In this analysis, the CASSCF wave function was initially constructed to obtain the starting set of orbitals for the localization procedure, after which the CASSCF optimized orbitals were localized by the Boys localization procedure.[44] Using the resulting localized MOs as a basis, a full CI with determinant level was performed to generate the electronic structures and their relative weights in the atomic orbital-like wave functions. These analysis were carried out along the intrinsic reaction coordinate of each reaction. The total energy, as calculated by the CI procedure, corresponds to that by the CASSCF calculation, and the relative weights of the electronic states having different CI configurations were expected to indicate the variations of electronic bond-forming or bond-breaking. The CI procedure is referred to hereafter as the CiLC−IRC method. For CI configurations, each bond was assigned by the terms of the singlet coupling and polarization, as shown in Scheme 3. In this scheme, the dotted line denotes a triplet coupling (antibonding) between the orbitals, and an ellipse denotes an ionic coupling (polarization). It was postulated that the singlet coupling and polarization terms could be describing the electronic structure of one bond, and that this description is related to a usual presentation by the valence bond (VB) theory. Interpretation using such an approach has been successful for interpreting some reaction mechanisms, as reported in previous papers.[12,38−43,45−48] Calculations for the CiLC−IRC analysis were performed using the GAMESS software package.[49] Other calculations were carried out using the Gaussian98 program.[50]

3. Results and Discussion

3.1. Geometry and Energy. Optimized geometries of the transition structures and products for the 10 reactions considered are displayed in Figure 1. When comparing the bond distances obtained by either CASSCF or B3LYP calculation levels, the difference for intermolecular distances of the transition structures is remarkable. In the case of the ONCH + HCX (X = CH, N, and P) system, the difference between the O−C bonds is rather large, amounting up to about 0.2 Å. The intermolecular bond distances for the transition structures obtained using the B3LYP method are in general longer than those using the CASSCF method, except for the O−N bond of the transition structure of the ONCH + NCH system. For the transition structure of the ONCH + NCH system, the CI coefficient of the main configuration using the CASSCF method is 0.822, which suggests that the transition state for ONCH + NCH system may possess a certain diradical character. To check the validity of

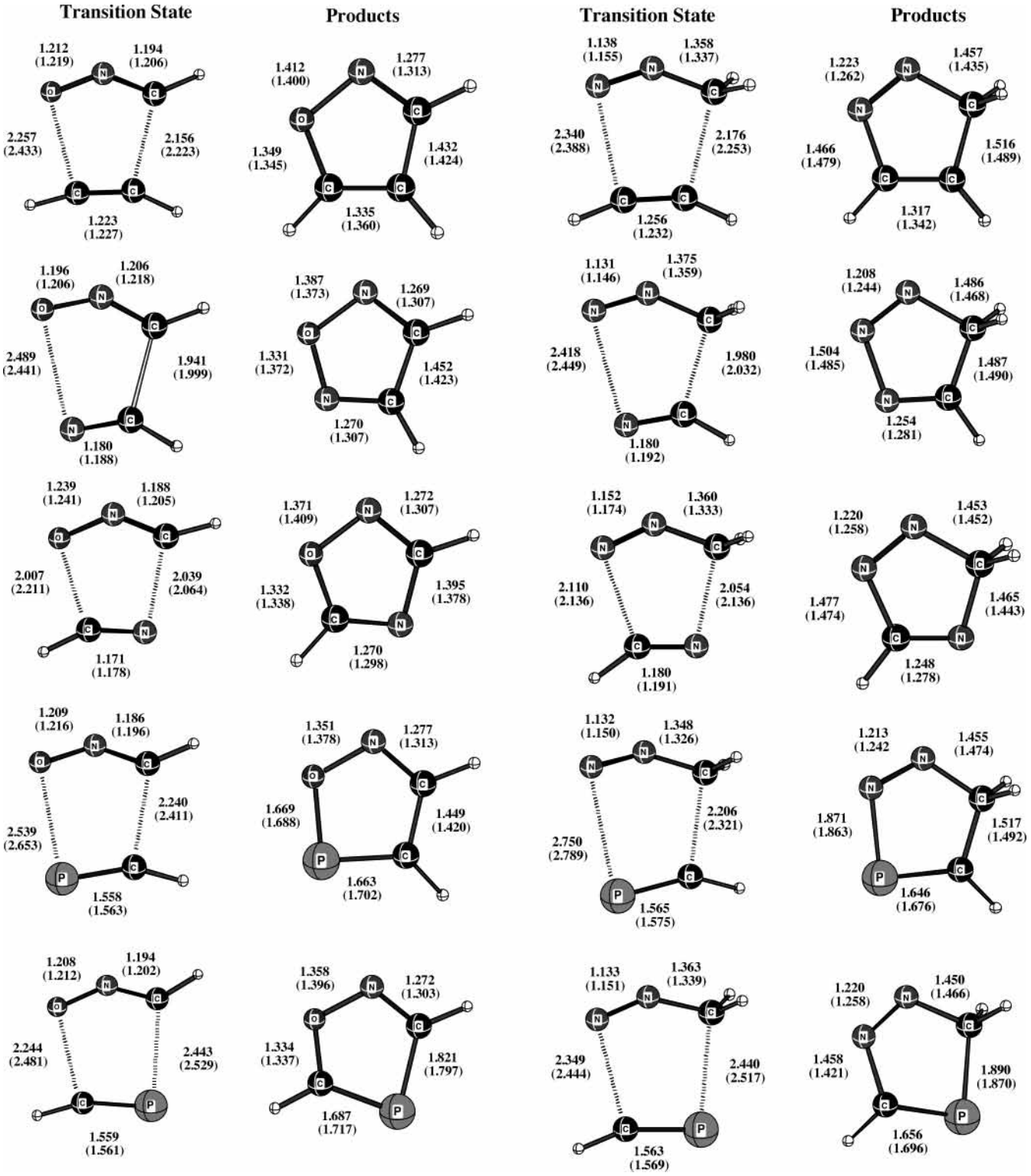

Figure 1. Geometrical parameters of the transition states and products of ONCH and $NNCH_2$ with HCCH, NCH, and PCH using the CASSCF/6-31G(d) and B3LYP/6-31G(d) methods. The B3LYP values are given in parentheses.

the B3LYP calculations, the total energy at the transition state was calculated by the unrestricted broken symmetry UB3LYP method. Our results showed comparable values for the total energy using the UB3LYP and the B3LYP methods. Accordingly, the UB3LYP calculations do not support the presence of a small diradical character, which corresponds to an estimation of a shorter O−N bond length by the B3LYP method. The short O−N bond arises thus from the smaller accuracy for describing a biradical state by the B3LYP method.

By comparing the bond distances of the newly formed bonds at the point of the transition state and their corresponding bonds of the products, the synchronous and asynchronous character of the relevant reaction could be determined. For the ONCH + XY systems, the formation of the C−Y bond is consistently earlier than that of the O−X bond at the transition structure, with the exception of the O−P bond formation. In the case of ONCH + PCH, the formation of the O−P and C−C bonds are almost synchronous at the transition state. Similarly, for the

TABLE 1: Relative Energies (kcal/mol) of the Transition States and Products from the Isolated Reactants for Reactions 1−10

	B3LYP	CASSCF	CAS-MP2	CCSD(T)
Reaction 1, ONCH + HCCH				
TS	12.1	25.7	17.1	13.4
product	−86.3	−90.2	−113.1	−81.6
Reaction 2, ONCH + NCH				
TS	19.4	35.3	23.5	22.2
product	−33.1	−16.5	−88.7	−27.3
Reaction 3, ONCH + HCN				
TS	13.9	30.9	16.6	15.5
product	−57.8	−46.8	−76.5	−54.1
Reaction 4, ONCH + PCH				
TS	6.4	18.6	8.1	6.1
product	−78.1	−66.9	−134.4	−76.7
Reaction 5, ONCH + HCP				
TS	5.5	19.1	7.8	5.5
product	−65.5	−54.9	−113.9	−62.8
Reaction 6, $NNCH_2$ + HCCH				
TS	14.5	25.5	14.8	15.4
product	−58.0	−44.7	−85.9	−53.8
Reaction 7, $NNCH_2$ + NCH				
TS	16.0	30.3	17.0	18.4
product	−15.3	−2.7	−57.3	−12.7
Reaction 8, $NNCH_2$ + HCN				
TS	20.2	34.9	18.2	22.2
product	−27.7	−13.2	−48.8	−24.4
Reaction 9, $NNCH_2$ + PCH				
TS	6.7	17.6	7.5	7.1
product	−41.0	−27.5	−99.2	−40.2
Reaction 10, $NNCH_2$ + HCP				
TS	5.7	17.0	3.6	5.8
product	−40.6	−25.5	−73.1	−38.5

$NNCH_2$ + XY systems, the C−Y bond formation is found to be more advanced than the N−X bond formation at the transition state, with the exception of the $NNCH_2$ + PCH system, in which the N−P bond formation is almost equal to the C−C bond formation. The formation of both new C−N bonds in the $NNCH_2$ + HCN system is nearly synchronous, which indicates that these bonds are formed at nearly the same time. In other words, when the Y atom, which reacts with the C atom of ONCH or $NNCH_2$, has a larger electronegativity than the X atom, the reaction occurs through a synchronous transition state. On the other hand, when the Y atom has smaller electronegativity than the X atom, the reaction proceeds through an asynchronous mechanism. These reaction mechanisms correspond well to the previously presented model.[11]

The relative energies for the stationary points are listed in Table 1. Consistent values for the energy barriers were obtained using the B3LYP, CAS-MP2, and CCSD(T) calculation levels, whereas energy barriers calculated using the CASSCF method are, as expected, over 10 kcal/mol higher than those using the other methods. For each dipole, the large differences of the activation energies depend on the dipolarophile molecules. The difference between the activation energies of ONCH and $NNCH_2$ reactions, for each dipolarophile, amounts to only a few kcal/mol. The activation energy for each dipolarophile molecule with the same 1,3-dipole (ONCH or $NNCH_2$) follows the order PCH < HCCH < NCH. This order corresponds to the lowest triplet excitation energies for PCH, HCCH, and NCH (based on the UB3LYP/6-31G(d) level: 86.9 kcal/mol for PCH, 136.6 kcal/mol for HCCH, and 159.2 kcal/mol for NCH). The excitation energies relate to the activation energies for the diradical state of dipolarophiles. The difference in the activation energies of reactions 4 and 5 is less than 1 kcal/mol and that of reactions 9 and 10 is about 1 kcal/mol, which indicates that effects of the regioselectivity for the PCH reaction systems are relatively minor, and may be related to the synchronous mechanism.

SCHEME 4

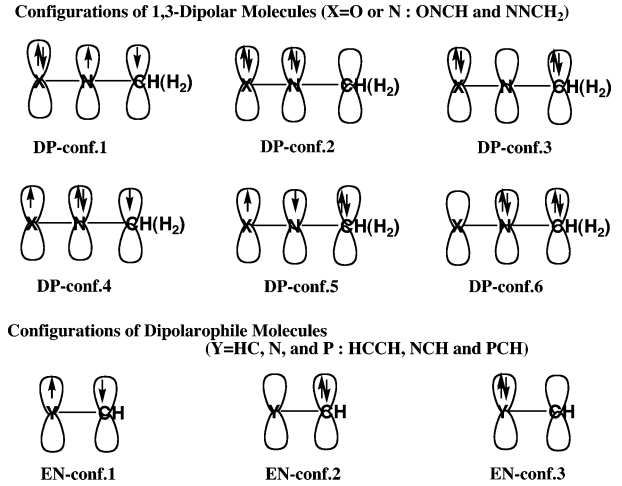

The energy barrier of reaction 2 is found to be higher by 4.4−6.9 kcal/mol than that of reaction 3. The activation energy barrier of reaction 7 is lower by 1.2−4.6 kcal/mol than that of reaction 8. The difference of the regioselectivity of the systems, including NCH, could probably be attributable to the difference of the mechanisms; this will be discussed in the following sections.

To unravel the electronic mechanisms of the 1,3-DC reactions, the CiLC−IRC calculations were performed for the reaction systems treated here.

3.2. CiLC−IRC Analysis. *3.2.1. ONCH + HCCH, NCH, and PCH Systems. (A) ONCH + HCCH.* Initially, the electronic structure of ONCH and HCCH was studied as isolated molecules by the CiLC method. For the CiLC analysis, three orbitals and four electrons for ONCH and two orbitals and two electrons for HCCH, correspond to the active orbitals in the reactions, were selected. The weights of the CI coefficients by the CiLC method for the isolated linear geometries of ONCH and HCCH and for each geometry taking part in the transition structure are listed in Tables 2 and 3, and their electronic configurations are shown in Scheme 4. The notations of "DP-conf.*n*" and "EN-conf.*n*" are assigned to the configurations of n-th for the 1,3-dipoles (ONCH and $NNCH_2$) and the dipolarophiles (HCCH, NCH, and PCH). The notations of "W(DP-conf.*n*)" and "W(EN-conf.*n*)" in Tables 2 and 3 refer to the weights of DP-conf.*n* and EN-conf.*n*, respectively. The notation of "bent" refers to the 1,3-dipole or dipolarophile structure part of the transition structure, whereas the notation of "Δ(L−B)" refers to the difference of the weights of each configuration between the linear and bent structures. The notations of "bent-1" and "bent-2" (and also B1 or B2 in Δ(L−B1) or Δ(L−B2)) stand for the dipolarophile geometries at the transition structures of Reactions 2 (or 4) and 3 (or 5), respectively. In the case of reactant ONCH (linear), DP-conf.1 is the major electronic state with weights of about 52% in all configurations, followed by the DP-conf.2 and DP-conf.4 states, each with weights of nearly 15%. For the structure of ONCH at the transition structure, the weights of DP-conf.1, DP-conf.2, and DP-conf.3 are decreased upon variation of the structure from the linear to the bent form. The configurations of DP-conf.1, DP-conf.2, and DP-conf.3 indicate the occupation of the lone pair electrons in the orbital of the

TABLE 2: Weights of the Configurations for ONCH and $NNCH_2$

	W(DP-conf.1)	*W*(DP-conf.2)	*W*(DP-conf.3)	*W*(DP-conf.4)	*W*(DP-conf.5)	*W*(DP-conf.6)
			ONCH			
(linear)	0.5174	0.1488	0.1094	0.1458	0.0756	0.0029
(bent)	0.4653	0.0811	0.0669	0.2899	0.0928	0.0040
Δ(L−B)	−0.052	−0.068	−0.043	0.144	0.017	0.001
			$NNCH_2$			
(linear)	0.3008	0.0443	0.1102	0.2932	0.2233	0.0282
(bent)	0.2906	0.0342	0.0590	0.4267	0.1689	0.0206
Δ(L−B)	−0.010	−0.010	−0.051	0.133	−0.054	−0.008

TABLE 3: Weights of the Configurations for XCH (X = HC, N, and P)

	W(EN-conf.1)	*W*(EN-conf.2)	*W*(EN-conf.3)
	HCCH		
(linear)	0.6699	0.1650	0.1650
(bent-ONCH)	0.7004	0.1605	0.1390
Δ(L−B)-ONCH	0.031	−0.005	−0.026
(bent-$NNCH_2$)	0.7080	0.1533	0.1387
Δ(L−B)-$NNCH_2$	0.038	−0.012	−0.026
	NCH		
(linear)	0.6688	0.1278	0.2034
(bent-1)	0.7178	0.1329	0.1494
Δ(L−B1)	0.049	0.005	−0.054
(bent-2)	0.6992	0.1257	0.1751
Δ(L−B2)	0.030	−0.002	−0.028
	PCH		
(linear)	0.7038	0.1835	0.1127
(bent-1)	0.7219	0.1771	0.1010
Δ(L−B1)	0.018	−0.006	−0.012
(bent-2)	0.7182	0.1754	0.1065
Δ(L−B2)	0.014	−0.008	−0.006

oxygen atom. The decrease of the weights of DP-conf.1, DP-conf.2, and DP-conf.3 could thus be attributed to the decrease of the lone pair of electrons of the oxygen atom of ONCH. On the other hand, the weight of DP-conf.4 is dramatically increased upon variation of the structure from a linear to a bent form. For the bent structure, the nature of the biradicals for both the oxygen and carbon sites is also markedly changed. Therefore, it can be considered that the electron motion from the lone pair orbital of the oxygen atom of ONCH to the orbital of the nitrogen atom occurs along the variation from a linear structure into a bent counterpart.

For the electronic structure of HCCH, the weight of EN-conf.1 turns out to increase upon the shift from the linear to the bent acetylene (in the transition structure) whereas the weights of the ionic configurations (especially DP-conf.3) is actually decreased. Increases in the weights were not observed for both ionic configurations (EN-conf.2 and EN-conf.3) in the bent structure. Consequently, the biradical character becomes remarkable during the bending of the CCH angle in HCCH.

From the results described above, it can be proposed that the mechanism of the cycloaddition reaction of ONCH and HCCH occurs through the coupling of the biradicals structures between both partners. On the basis of such findings derived from the electronic structure of the isolated molecules, the mechanisms of ONCH and HCCH were studied using the CiLC−IRC method.

The mechanisms of the 1,3-DC of ONCH with HCCH have been presented in a previous paper,[11,12] and for comparative purposes, the results are outlined hereafter. The weights of the CI coefficients along the IRC pathway, as determined by the CiLC−IRC method, are shown in Figure 2 (weights with values <0.001 were not included). Some of the configurations with larger CI coefficients are displayed in Scheme 5. The largest variation of the configuration weights are observed for the decrease of configuration 1 and the increase of configuration 7, from the direction of reactants to products. These two configurations, which cross each other at the region of the transition state, are the main configurations for the reactants and the products, respectively. It is reasonable to assume that the reaction of this system is induced by the electron movement from the oxygen atom of ONCH to the nitrogen atom, which corresponds to the proposed basic mechanism derived from the electronic structure of isolated molecules, as mentioned above. The variation of the second largest weight of the configurations, as shown in configurations 2 and 45, can be considered as being composed from two singlet coupling terms. Specifically, configuration 2 is composed from the singlet coupling terms of the N−C and C−C bonds of acetylene. The polarization terms corresponding to the singlet coupling terms of these two bonds are configurations 5 and 6 and configurations 3 and 4, respectively. Configuration 2 can also be considered as the antibonding of the main configurations of ONCH and HCCH (DP-conf.1 and EN-conf.1). Configuration 45 is composed from the singlet coupling terms of the new O−C and C−C bonds. The weight of configuration 3 is larger than that of configuration 4 when proceeding from the reactant side to the transition state region, and the weight of configuration 5 is larger than that of configuration 6.

These results indicate that one of the acetylene carbon atoms possesses an anionic nature at the transition state region, and the ONCH carbon atom possesses a cationic nature. Consequently, the other acetylene carbon atom has a cationic character.

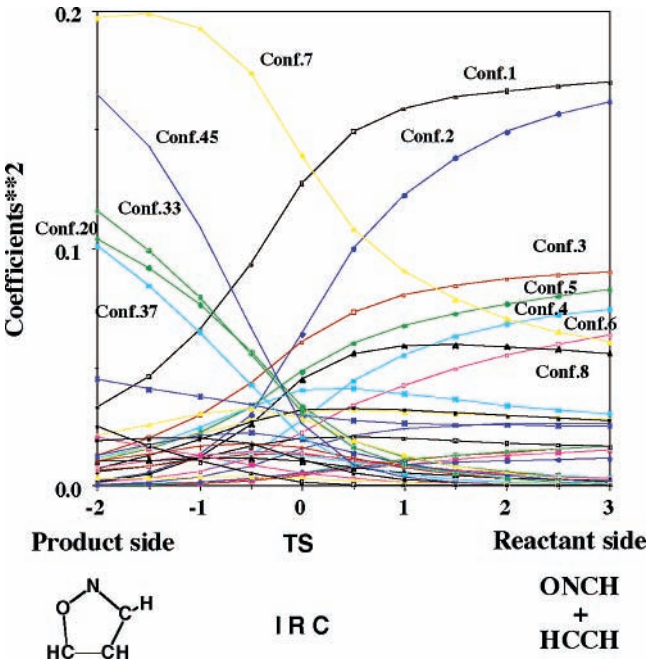

Figure 2. Weights of the CI coefficients of the CiLC calculations along the IRC pathway of the cycloaddition reaction of ONCH and HCCH. The units of IRC are bohr × $amu^{1/2}$.

SCHEME 5: Selected Electronic Configurations for CiLC Analysis[a]

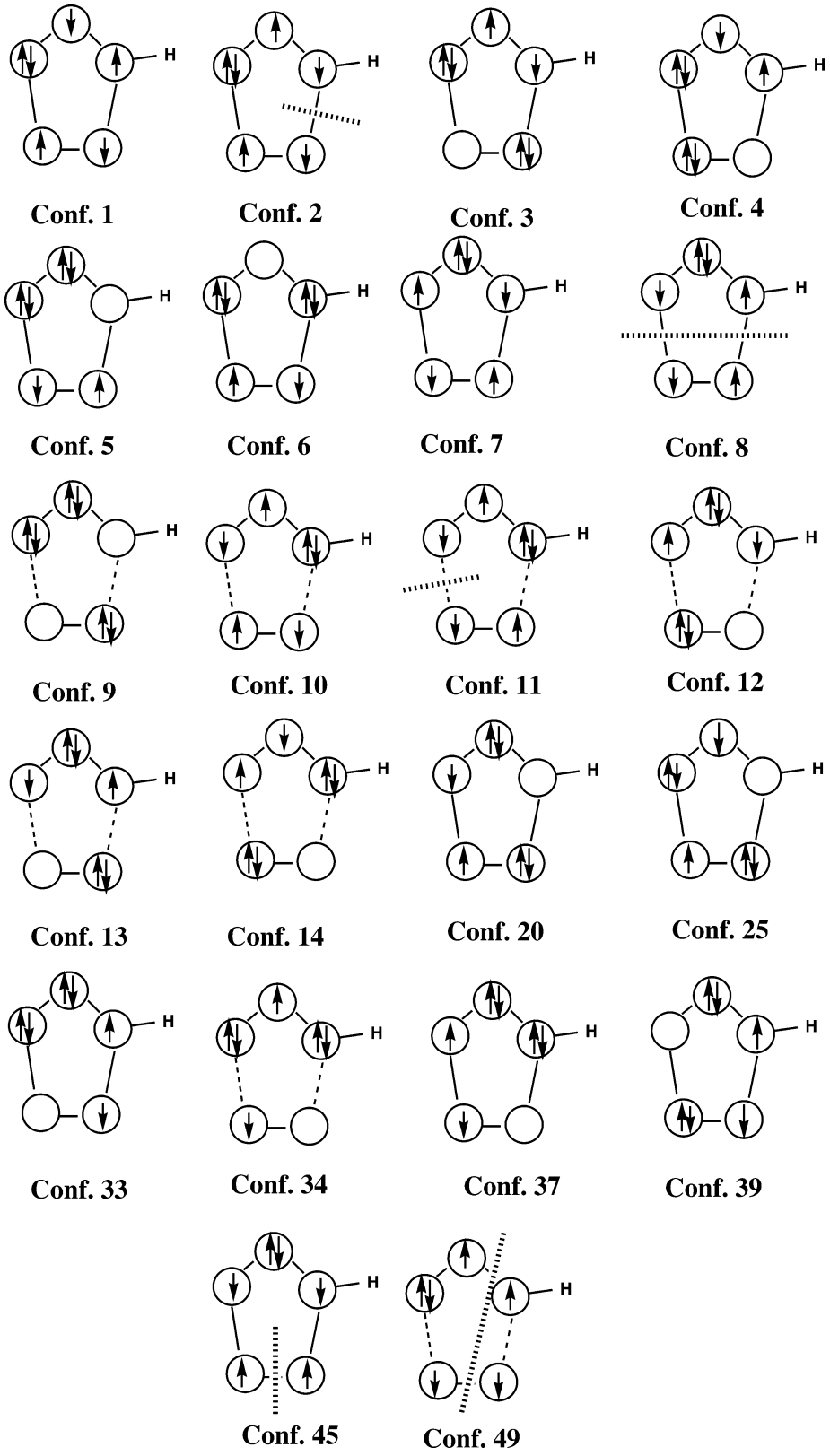

[a] Dotted lines denote triplet coupling (antibonding) between orbitals

The polarization terms corresponding to the singlet coupling terms for the two bonds for configuration 45 are those of configuration 33 and of configurations 20 and 37. The weight of configuration 20 is larger than that of configuration 37 at the transition state region. The difference in weights corresponds to the electronic structure of the C−C bond between one acetylene carbon atom and the ONCH carbon atom at the transition point. It also corresponds to that of the C−O bond between the other carbon atom of acetylene and the oxygen atom of ONCH. Although the reaction mechanism is best characterized as a concerted biradical coupling, the four active sites may be slightly polarized, as shown in below. Overall,

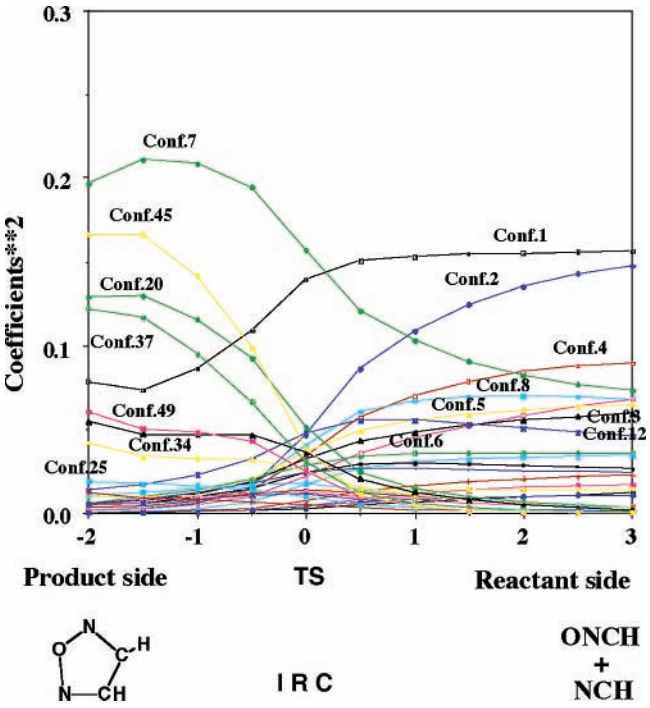

Figure 3. Weights of the CI coefficients of the CiLC calculations along the IRC pathway of the cycloaddition reaction of ONCH and NCH. The units of IRC are bohr × amu$^{1/2}$.

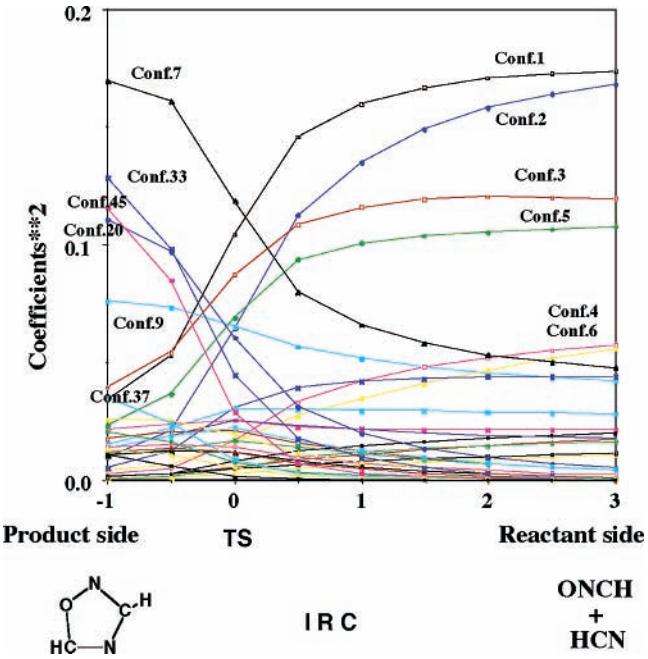

Figure 4. Weights of the CI coefficients of the CiLC calculations along the IRC pathway of the cycloaddition reaction of ONCH and HCN. The units of IRC are bohr × amu$^{1/2}$.

this mechanism corresponds to the results presented in our previous paper.[11]

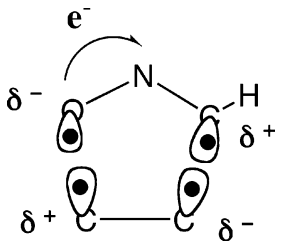

(B) ONCH + NCH. The weights of the CI coefficients along the IRC pathway of the 1,3-DC of ONCH with NCH are displayed in Figures 3 and 4. It is important to note that the reaction is regioselective defined by two distinct reactions 2 and 3. For reaction 2 in Figure 3, the variations of the weights of configurations 1, 2, and 7 are similar to those of the corresponding configurations in the ONCH + HCCH reaction. The weight of configuration 1 does not change significantly in the region between the reactant and transition state. For the reactant side, the weight of configuration 3 is very small due to the polarity of NCH molecule. For the product side, the variations of the weights of configurations 7, 45, 20, and 37 are significant. Configuration 7 is the main configuration for the product whereas configuration 45 can be considered as the singlet coupling terms for the new O−N and C−C bonds. For configuration 45, the weights of the two bonds are not distinguishable. Configurations 20 and 37 indicate the polarization terms of the new C−C bond, and as a consequence, it could be considered that the reaction, after the transition state is passed, proceeds through a rather asynchronous mechanism. This result corresponds to those of previous studies that were based on geometrical parameters, namely the transition state has a diradical character for the oxygen atom in ONCH and the nitrogen atom in NCH. For the reaction of ONCH with NCH of reaction 2, as shown in Figure 3, configurations with large weights cross each other near the transition state region. This pattern is similar to that of Diels−Alder reaction of butadiene with ethylene, as previously reported,[41] and indicates that the reaction follows a more synchronous mechanism at the transition state region from the reactant side, and after the transition state has passed, the reaction follows a more asynchronous mechanism.

For the reaction 3 of ONCH + HCN shown in Figure 4, the main configurations 1 and 7 also cross each other at the transition state region. The weight of configuration 2 corresponding to the singlet coupling terms of the C−N bonds (old π-bonds) in HCN and ONCH is decreased from reactant to product and crosses at the transition state region with that of configuration 45. The latter corresponds to the singlet coupling terms of the new O−C and C−N bonds. The weights of configurations 3 and 5 remain nearly unchanged before reaching the transition state region from reactants. The weights of configurations 4 and 6 decrease monotonically. While configurations 3 and 4 correspond to the polarization terms of the C−N bond (old π-bond) in HCN, configurations 5 and 6 correspond to the polarization terms of the N−C bond (old π-bond) in ONCH. This means that both N−C bonds are polarized to the NCH nitrogen atom and the fulminic acid carbon atom. On the other hand, the weights of configurations 33 and 20 are increased from transition state region to product side; configurations 33 and 20 correspond to the polarization terms of the new O−C and C−N bonds, respectively. At the region of transition state, the weights of configurations 20 and 33 are significantly larger than that of configuration 45. Accordingly, the reaction between ONCH and HCN of reaction 3 is likely occurring through an ionic electrocyclic mechanism, as shown below. The weights of the configurations of the two old C−N and N−C bonds approach those of the two new O−C and C−N bonds near transition state region, and therefore, reaction 3 between ONCH and HCN is apparently occurred following a concerted synchronous (ionic electrocyclic) mechanism (mechanism II, Scheme 1).

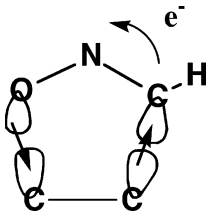

(C) ONCH + PCH. The weights of the CI coefficients along the IRC pathway of the reactions between ONCH and PCH were also calculated (see Supporting Information). Again, this reaction is regioselective, manifested by both reactions 4 and 5. For reaction 4, the variations of the weights of the CI coefficients along the IRC path are very similar to those for the ONCH + HCCH system (with an exception of the small weight of configuration 4). Although configuration 4 describes the polarization term of PCH (the electrons localization to the orbital of the phosphorus atom), the electrons are rather centered at the carbon atom for the P−C bond because of the difference in electronegativities of carbon and phosphorus atoms. The difference between the two polarization terms of the P−C bond is also observed from the weights of EN-conf.2 and EN-conf.3, as shown in Table 3. The main configurations (configurations 1 and 7) for the reactant and product sides cross at the transition state region. The variation of the second largest weight (configuration 2) again corresponds to the singlet coupling terms of the C−N bond of ONCH. The P−C bond is calculated to be decreased from reactants to transition state region with a decreasing of their polarization terms (configurations 3−6). On the other hand, the singlet coupling terms (configuration 45) of both novel O−P and C−C bonds tend to increase from transition state region to product side with increasing polarization terms (configurations 20, 33, and 37). This reaction, therefore, occurs through the typical synchronous mechanism as reaction 1.

The variations of the weights of the CI coefficients along the IRC path of reaction 5 are also similar to those of the ONCH + HCCH system. In comparison with the results described above for reaction 4, the polarization term (configuration 4) of PCH is now larger than the other side polarization term (configuration 3) of PCH, which can again be attributed to the difference in electronegativities of both carbon and phosphorus atoms. The influence on the weights of the configurations by the electronegativities of the carbon and phosphorus atoms is also observed for the polarization terms of the two novel C−O and P−C bonds in the product.

The essential reaction mechanisms of reactions 4 and 5, however, could be depicted by the following steps. Along the IRC pathway, the weight of configuration 1 becomes decreased with an increasing weight of configuration 7; this is namely, an electron in the lone pair orbital of the oxygen atom of ONCH moves into an orbital of the nitrogen atom. This actually corresponds to the basic mechanism derived from electronic structure of the isolated molecules. With such an electron motion, the N−C bond becomes weaker, as shown in the decreased weights of configurations 5 and 6 (polarization terms of the N−C bond). After the transition state is passed, the two new bonds were formed rapidly and almost synchronously.

3.2.2. $NNCH_2$ + HCCH, NCH, and PCH Systems. (A) $NNCH_2$ + HCCH. Results collected using the CiLC method on the electronic structure of isolated diazomethane $NNCH_2$, with some geometrical parameters, have been described in a previous section. The weights of the CI coefficients obtained by the CiLC method for the isolated geometry (NNC:linear) of $NNCH_2$ and the $NNCH_2$ geometry part (bent) of the transition state ($NNCH_2$ + HCCH) are listed in Table 2. The configurations are displayed in Scheme 4. The electronic structure of linear $NNCH_2$ (reactant) is the resonance state of three major configurations (DP-conf.1, DP-conf.4, and DP-conf.5). It is worth noting that the weight of DP-conf.1 is almost identical to that of DP-conf.4. The electronic structure of $NNCH_2$ is more similar to that of $NNCH_2$ part in the product (cyclic compound) than that in the case of ONCH. The weights of DP-conf.3 and DP-conf.5 of $NNCH_2$ are decreased upon bending, whereas the weight of DP-conf.4 increased. The variation of the weights of these configurations in going from the linear to the bent structure implies that the electrons in the orbital of the $NNCH_2$ carbon atom are decreased, whereas those in the orbital of the $NNCH_2$ central nitrogen atom are increased. The movement of the $NNCH_2$ electrons for the bending significantly differs from that of ONCH. The weights of the CI coefficients for the HCCH bent structure (bent-$NNCH_2$), corresponding to the structure of HCCH at the transition state, are listed in Table 3. Following bending, the weight of EN-conf.1 is increased; in contrast, the ionic configurations are decreased. Since the decrease of the weight of EN-conf.2 for this bent structure is larger than that of the bent-ONCH, the reaction of $NNCH_2$ + HCCH is a late transition state, as compared with that of ONCH + HCCH. It is also reasonable to suggest that the electronic mechanisms of the 1,3-DC reaction of $NNCH_2$ + HCCH occurred through the coupling of the biradical structures for both molecules with the electron movement in $NNCH_2$ from the carbon atom to the central nitrogen atom.

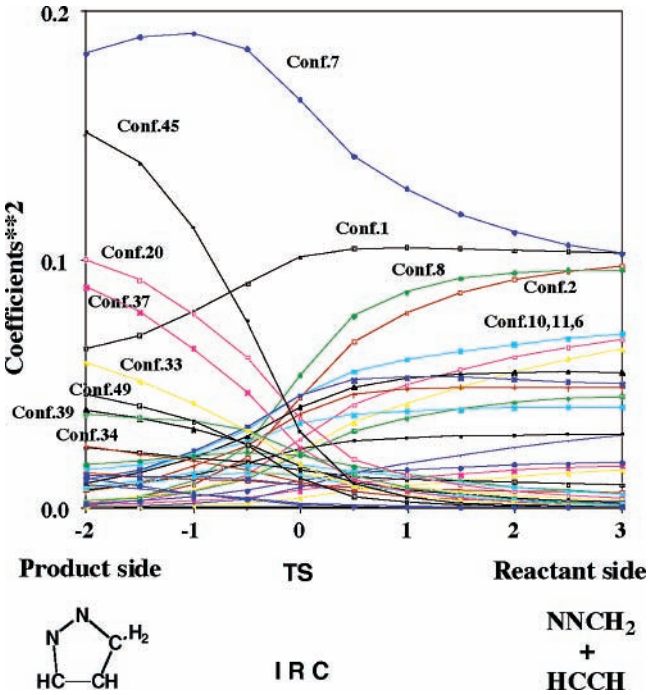

Figure 5. Weights of CI coefficients of CiLC calculation along the IRC pathway of the cyclic reaction of $NNCH_2$ and HCCH. The units of IRC are bohr × $amu^{1/2}$.

For a in-depth study of the variations of electronic structure, the weights of the CI coefficients along the IRC pathway were determined by the CiLC−IRC method, as shown in Figure 5. The largest variation of the configuration weights was observed for an increase in configuration 7, from reactant to product. The increasing weight of configuration 7 corresponds to the variation of DP-conf.4 between the linear and bent geometries of $NNCH_2$. The weight of configuration 2, which is associated with an anticoupling between DP-conf.1 of $NNCH_2$ and EN-conf.1 of HCCH, is decreased along the pathway. Similarly, the weight

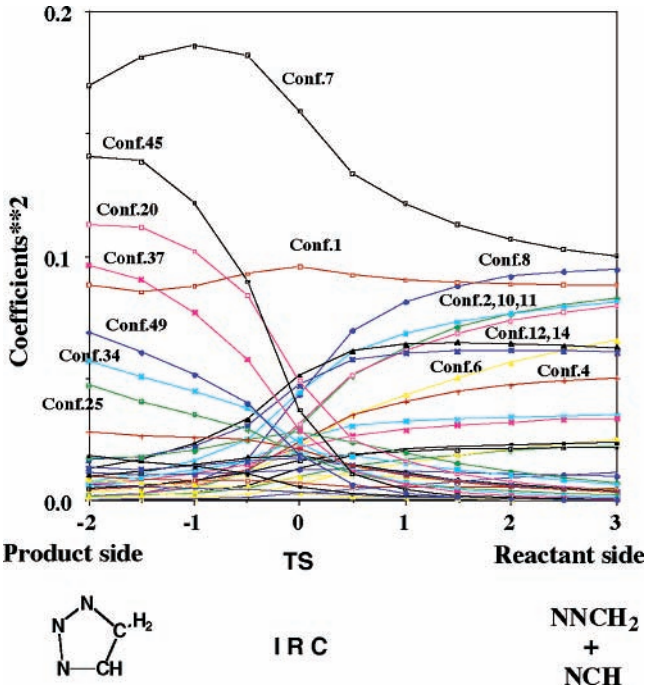

Figure 6. Weights of CI coefficients of CiLC calculation along the IRC pathway of the cyclic reaction of $NNCH_2$ and NCH. The units of IRC are bohr × $amu^{1/2}$.

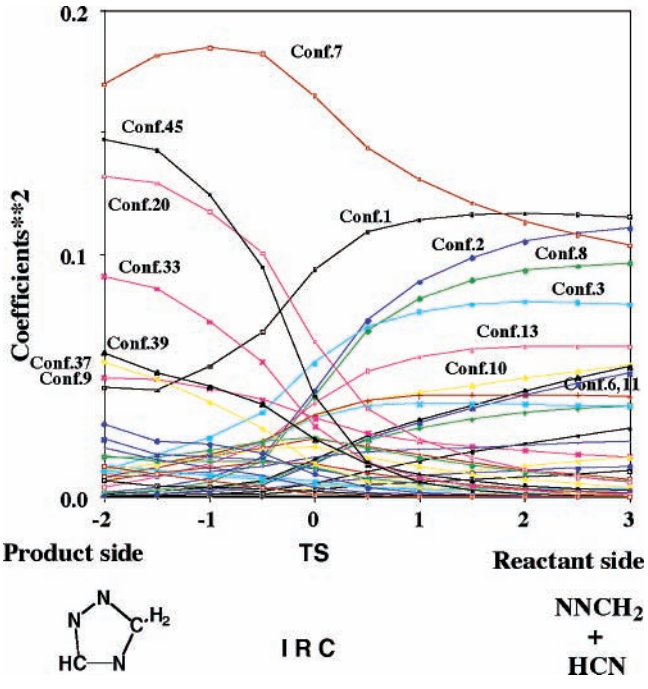

Figure 7. Weights of CI coefficients of CiLC calculation along the IRC pathway of the cyclic reaction of $NNCH_2$ and HCN. The units of IRC are bohr × $amu^{1/2}$.

of configuration 8, which is related to the anticoupling between DP-conf.4 of $NNCH_2$ and EN-conf.1 of HCCH, is also decreased. The weights of configurations 10, 11, and 6 are all decreased, corresponding to a variation of those of DP-conf.3 and DP-conf.5 between the diazomethane linear and bent geometries. The weight of configuration 1 is not changed until the transition state region is reached; the variations in the weights of the configuration from the reactants actually corresponds to the basic mechanism considered solely from the isolated $NNCH_2$ and HCCH. Proceeding from the product, an increase in the weight of configuration 33 is less important than those of configurations 20 and 37, which indicates that the reaction is more asynchronous than that of ONCH + HCCH.

From the above results, it could be proposed that the 1,3-DC reaction between $NNCH_2$ and HCCH occurs through a biradical coupling between both partners with an electron movement within $NNCH_2$ in going from the terminal carbon to the central nitrogen atom.

(B) $NNCH_2$ + NCH. The weights of the CI configurations along the IRC pathways of the reaction between NCH_2 and NCH are displayed in Figures 6 and 7. Again both reactions 7 and 8 are the two components of a regioselective reaction. For reaction 7 summarized in Figure 6, the variations of the weights of configurations 7, 8, 2, 10, and 11 are similar to those in the reaction between $NNCH_2$ and HCCH. The weight of the antibonding coupling (configuration 8) between DP-conf.4 of $NNCH_2$ and EN-conf.1 of NCH is consistently decreased along the IRC pathway, whereas the weight of the bonding coupling (configuration 7) is uniformly increased. Furthermore, the weights of the antibonding coupling (configuration 2) between DP-conf.1 of $NNCH_2$ and EN-conf.1 of NCH are also decreased. Decrease in the weights of configurations 10 and 11 and increase in that of configuration 7 point out an electron movement within $NNCH_2$, from the terminal carbon atom to the central nitrogen. For the weight of configuration 1, the variation from reactants to transition state region is mostly similar to that in the $NNCH_2$ + HCCH system. From transition state to product, the weight is not significantly modified. For the cyclic product, increases in the weights of configurations 45, 20, and 37 imply the formation of the two new C−C bonds. Although configuration 45 may include the singlet coupling term of a new N−N bond, the weight of the polarization terms (configurations 33 and 39) of the N−N bond is significantly smaller than that of the C−C bond (configurations 20 and 37). Increases in the weights of configuration 49 and 34 also emphasize a new C−C bond formation, without the variation of the weight of configuration 1. The reaction process, therefore, occurs through a typical asynchronous mechanism.

For reaction 8, $NNCH_2$ + HCN illustrated in Figure 7, the variations of the weights of configurations 1, 2, 7, and 8 are almost similar to those of the reaction $NNCH_2$ + HCCH. The weights of configurations 3 and 13, which suggest a polarization of the C−N bond in HCN, remain almost unchanged in going from reactants to transition state. For the product, increases in the weights of configurations 45 and 20 imply a bond formation of a $C(H_2)$−N(CH) bond, whereas increases in the weights of configurations 45 and 33 manifest a N(−N)−*C*(*H*) bond formation. The fact that the weight of configuration 20 is significantly larger than that of configuration 45 at the transition state region suggests a reaction presumably occurring through an ionic electrocyclic mechanism, similar to that of reaction 3. In other words, the reaction proceeds via a mechanism with a slightly asynchronous character. Differences in the regioselectivities for reactions 7 and 8 could be accounted for by the diradical- and ionic-coupling mechanisms.

(C) $NNCH_2$ + PCH. The weights of the CI coefficients along the IRC pathways of the 1,3-DC of $NNCH_2$ + PCH were also calculated (see Supporting Information). Reactions 9 and 10 correspond to the two pathways that determine the regioselectivity of this addition. For reaction 9, the variations of the weights of configurations from reactants to transition state are very similar to those of the reaction $NNCH_2$ + HCCH. Increased weights are observed for configurations 45, 20, and 37 from transition state region to product side. Consistent increase in the weights of configurations 45, 20, and 37 demonstrates the formation of a C−C bond under the electronic condition of DP-

conf.4 of $NNCH_2$. The weights of configurations 49, 34, and 25 are increased from transition state region to product. The configuration set [49,34,25] could be described as the C−C bond under the electronic condition of DP-conf.1 of $NNCH_2$; namely, the C−C bond is formed under the electronic condition of DP-conf.1 and DP-conf.4 of $NNCH_2$, thus indicating a strong asynchronous mechanism.

For reaction 10, variations in the weights of the configurations from reactants to transition state are also similar to those of reaction 9. In comparison with the latter, the weight of configuration 1 turns out to be decreased from transition state to product. The weights of configurations 45, 37, and 20 are now increased in the same direction and thus suggest a C−P bond formation. Increases in the weights of configurations 33 and 39 are also observed for the same region. Configuration set [45,33,39] is no doubt associated with a new N−C bond formation under the electron condition of DP-conf.4 of $NNCH_2$. Along the IRC pathway, increasing weights of configuration set [45, 33, 39] are detected later than those for configuration set [45, 37, 20]. This indicates a mechanism possessing a slightly asynchronous character.

3.3. Discussion. As shown above, the 1,3-DC reactions can be specified using three characteristics: First, the electron movement within the 1,3-dipole occurs during the initial process from the reactants to the transition state region. Second, a diradical coupling or ionic mechanisms for an addition process between both 1,3-dipole and dipolarophile partners takes place. It is important to note that the first process is inherently related to the second one; namely, when the intramolecular electron movement occurs in the 1,3-dipole, the second process has to be a diradical coupling. For reactions involving the ONCH system, the electron movement occurs from the oxygen to nitrogen atom, and producess a biradical state for the 1,3-dipole (ONCH), with the exception of reaction 3. For the reactions of the $NNCH_2$ system, the electron movement starts within $NNCH_2$ from the carbon to the central nitrogen atom, with the exception of reaction 8. The mechanism for reactions 3 and 8 is an ionic process (electrocyclic). For the cases characterized by a large difference in electronegativities of the two dipolarophile atoms and the suitable approach with the 1,3-dipolar molecule, the reaction proceeds through an ionic electrocyclic mechanism. Third, the mechanism involves a synchronous or asynchronous process for the region of the transition state and/or after the transition state. The process of synchronity or asynchronity is closely related to the activation energy for both the mechanisms of ionic electrocyclic and diradical coupling. Accordingly, we can classify the 10 reactions as ionic electrocyclic or diradical coupling mechanisms. The ionic electrocyclic mechanism includes reactions 3 and 8. According to the electronegativities of the atoms, the conformation at the transition state of reaction 3 occurred more readily than that of reaction 8. This is in line with the difference in activation energies between reactions 3 and 8. In fact, the activation barriers of reaction 3 are calculated to be lower by about 2 and 7 kcal/mol than those of reaction 8. The diradical coupling mechanism includes other all reactions.

On the basis of the CASSCF and CAS-MP2 methods, for the diradical coupling mechanism for the same dipolarophile, reactions including ONCH consistently have higher activation energies than those involving $NNCH_2$; this observation can be understood from the electronic states of the isolated ONCH and $NNCH_2$. On the other hand, calculations based on the B3LYP and CCSD(T) methods resulted in lower activation energies for reactions that include ONCH than those that include $NNCH_2$, with the exception for reactions 2 and 7. This is attributable to the difference between the single determinant level and the multireference level calculations of the quantum chemical methods.

4. Conclusions

The 1,3-dipolar cycloaddition reaction mechanisms of ONCH and $NNCH_2$ with HCCH, NCH, and PCH dipolarophiles could be classified using the CiLC−IRC analysis on the basis of ab initio multireference wave functions. These reactions are governed by "chameleonic" mechanisms as in the Cope rearrangement. The mechanisms of the reactions can roughly be classified as ionic electrocyclic or diradical coupling. The ionic electrocyclic mechanism is expected in the cases that involve favorable approaxhes for mechanism III in Scheme 1, identified by a large difference between the electronegativities of the participating atoms (especially the dipolarophile molecule). For the diradical coupling mechanism, the first process is an intramolecular electron movement within the 1,3-dipole—from the oxygen to the nitrogen atom of ONCH and from the carbon to the central nitrogen atom of $NNCH_2$. The resulting activation energy for the whole transformation is essentially related to the excitation energy of the diradical state of the dipolarophile. For the same dipolarophile, the activation energy is determined by the electron movement of its 1,3-dipolar counterpart. For systems having the same mechanism, the synchronous or asynchronous characters of the reaction are also related to the activation energies. In real systems, it can be expected that the asynchronous character of a 1,3-DC is defined as a deviation of the above two types of mechanisms.

Acknowledgment. S.S. thanks the Ministry of Education, Science, and Culture of Japan for the Grant-in-Aid. M.T.N. thanks the KU Leuven Research Council for continuing support (GOA program). Computer time was made available by the Computer Center of the Institute for Molecular Science and Osaka Sangyo University using an SGI Power Challenge computer.

Supporting Information Available: Figures showing weights of the CI coefficients of the CiLC calculation along the IRC pathway of the cycloaddition reactions of ONCH and PCH, ONCH and HCP, $NNCH_2$ and PCH, and NNCH2 and HCP. This material is available free of charge via the Internet at http://pubs.acs.org.

References and Notes

(1) Padwa, A., Ed. *1,3-Dipolar Cycloaddition Chemistry*; Wiley-Interscience: New York, 1984; Vols. 1 and 2.
(2) Gothelf, K. V.; Jorgensen, A. *Chem. Rev.* **1998**, *98*, 863.
(3) Suser, J.; Sustmann, R. *Angew. Chem., Int. Ed Engl.* **1980**, *19*, 779.
(4) Houk, K. N.; Li, Y.; Evanseck, J. D. *Angew. Chem., Int. Ed Engl.* **1992**, *31*, 682.
(5) Dewar, M. J. S.; Caoxian, J. *Acc. Chem. Res.* **1992**, *25*, 537.
(6) Firestone, R. A. *J. Org. Chem.* **1968**, *33*, 2285.
(7) Firestone, R. A. *J. Org. Chem.* **1972**, *37*, 2181.
(8) Huisgen, R. J. *J. Org. Chem.* **1976**, *41*, 403.
(9) Sakata, K. *J. Phys. Chem. A* **2000**, *104*, 10001.
(10) Harcourt, R. D.; Schulz, A. *J. Phys. Chem. A* **2000**, *104*, 6510.
(11) Nguyen, M. T.; Chandra, A. K.; Sakai, S.; Morokuma, K. *J. Org. Chem.* **1999**, *64*, 65.
(12) Nguyen, M. T.; Chandra, A. K.; Uchimaru, T.; Sakai, S. *J. Phys. Chem. A* **2001**, *105*, 10943.
(13) Karadakov, P. B.; Cooper, D. L.; Gerratt, J. *Theor. Chem. Acc.* **1998**, *100*, 222.
(14) Leroy, G.; Sana, M.; Burke, L. A.; Nguyen, M. T. In *Quantum Theory of Chemical Reactions*; Daudel, R., et al., Eds.; D. Reidel; Dordrecht, The Netherlands, 1979; Vol.1, p 91.
(15) Sana, M.; Leroy, G.; Dive, G.; Nguyen, M. T. *J. Mol. Struct. (THEOCHEM)* **1982**, *89*, 147.

(16) Daudel, R.; Leroy, G.; Peeters, D.; Sana, M. *Quantum Chemistry*; Wiley: New York, 1983.
(17) Ruedenberg, K.; Schmidt, M. W.; Gilbert, M. M.; Elbert, S. T. *Chem. Phys.* **1982**, *71*, 41.
(18) Ruedenberg, K.; Schmidt, M. W.; Gilbert, M. M. *Chem. Phys.* **1982**, *71*, 51.
(19) Ruedenberg, K.; Schmidt, M. W.; Gilbert, M. M.; Elbert, S. T. *Chem. Phys.* **1982**, *71*, 65.
(20) Cundari, T. R.; Gordon, M. S. *J. Am. Chem. Soc.* **1991**, *113*, 5231.
(21) Sakai, S. *J. Phys. Chem. A* **1997**, *101*, 1140.
(22) Chandra, A. K.; Nguyen, M. T. *J. Phys. Chem. A* **1998**, *102*, 6181.
(23) Chandra, A. K.; Nguyen, M. T. *J. Comput. Chem.* **1998**, *19*, 195.
(24) Leroy, G.; Sana, M. *Tetrahedron* **1975**, *31*, 2091.
(25) Blavins, J. J.; Karadakov, P. B.; Cooper, D. L. *J. Org. Chem.* **2001**, *66*, 4285.
(26) Roos, B., Lawley, K. P., Ed. *Advances in Chemical Physics*; Wiley: New York, 1987; Part II, Vol. 69, p 399.
(27) Hariharan, P. C.; Pople, J. A. *Theor. Chim. Acta* **1973**, *28*, 213.
(28) Gordon, M. S. *Chem. Phys. Lett.* **1980**, *76*, 163.
(29) McDouall, J. J.; Peasley, K.; Robb, M. A. *Chem. Phys. Lett.* **1988**, *148*, 183.
(30) Raghavachari, K.; Trucks, G. W.; Pople, J. A.; Head-Gordon, M. *Chem. Phys. Lett.* **1989**, *157*, 479.
(31) Dunning, T. H., Jr. *J. Chem. Phys.* **1989**, *90*, 1007.
(32) Kendall, R. A.; Dunning, T. H., Jr.; Harrison, R. J. *J. Chem. Phys.* **1992**, *96*, 6769.
(33) Woon, D. E.; Dunning, T. H., Jr. *J. Chem. Phys.* **1995**, *103*, 4572.
(34) Becke, A. D. *Phys. Rev. A* **1988**, *38*, 3098.
(35) Lee, C.; Yang, W.; Parr, R. G. *Phys. Rev. B* **1988**, *37*, 785.
(36) Fukui, K. *J. Phys. Chem.* **1970**, *74*, 4161.
(37) Ishida, K.; Morokuma, K.; Komornicki, A. *J. Chem. Phys.* **1977**, *66*, 2153.
(38) Sakai, S. *Int. J. Quantum Chem.* **1998**, *70*, 291.
(39) Sakai, S. *J. Mol. Struct. (THEOCHEM)* **1999**, *461*−*462*, 283.
(40) Sakai, S.; Takane, S. *J. Phys. Chem. A* **1999**, *103*, 2878.
(41) Sakai, S. *J. Phys. Chem. A* **2000**, *104*, 922.
(42) Sakai, S. *Int. J. Quantum Chem.* **2000**, *80*, 1099.
(43) Sakai, S. *J. Phys. Chem. A* **2000**, *104*, 11615.
(44) Foster, J. M.; Boys, S. F. *Rev. Mod. Phys.* **1960**, *32*, 300.
(45) Sakai, S. *J. Mol. Struct. (THEOCHEM)* **2002**, *583*, 181.
(46) Sakai, S. *Int. J. Quantum Chem.* **2002**, *90*, 549.
(47) Lee, P. S.; Sakai, S.; Horstermann, P.; Roth, W. R.; Kallel, E. A.; Houk, K. N. *J. Am. Chem. Soc.* **2003**, *125*, 5839.
(48) Sakai, S. *J. Mol. Struct. (THEOCHEM)* **2003**, *603*, 177.
(49) Schmidt, M. W.; Buldridge, K. K.; Boatz, J. A.; Jensen, J. H.; Koseki; Gordon, M. S.; Nguyen, K. A.; Windus, T. L.; Elbert, S. T. *QCPE Bull.* **1990**, *10*, 52.
(50) Frisch, K. J.; Trucks, G. W.; Schlegel, H. B.; Gill, P. M. W.; Johnson, B. G.; Robb, M. A.; Cheseman, J. R.; Keith, T. A.; Petersson, G. A.; Montgomery, J. A.; Raghavachari, K.; Al-Laham, M. A.; Zakrzewski, V. G.; Ortiz, J. V.; Foresman, J. B.; Cislowski, J.; Stefanov, B. B.; Nanayakkara, A.; Challacombe, M.; Peng, C. Y.; Ayala, P. Y.; Chen, W.; Wong, M. W.; Andres, J. L.; Replogle, E. S.; Comperts, R.; Martin, R. L.; Fox, D. J.; Binkley, J. S.; DeFrees, D. J.; Baker, J.; Stewart, J. P.; Head-Gordon, M.; Gonzalez, C.: Pople, J. A. Gaussian 98. Gaussian, Inc.: Pittsburgh, PA, 1998.